High Surface Area Graphite

On one hand, the fact that tri-unsaturated FAEE may be sensitive to temperature together with a new reactor design which allowed us to work in vapour phase at lower temperatures, made easier the study of the activity testing at lower temperature. On the other hand, another carbonaceous material with different textural and surface-chemistry properties was studied. The chosen material was high surface area graphite (HSAG).

The relatively high values of hydrogenation selectivity obtained when using AC as a catalyst suggested that hydrogen spill-over related to the microporous structure might be the responsible for the obtaining of mono-unsaturated FAEE. Therefore, the choice of a non-microporous material, such as the HSAG-100, was justified.

Once more, a reference to the work carried out by Figueiredo et al. [1,2] and Schlögl et al. [3-5] is relevant when introducing graphitic catalysts in dehydrogenation reactions.

HSAG-100 was used as a catalyst and its catalytic activity was studied at 200 °C. Once again, two reactor configurations (old and new, see *Chapter 2.1*) were compared.

3.8.1 Experimental

The catalytic tests were performed at 200 °C with feed of 0.055 μmol g_{cat}^{-1} s^{-1} using argon as inert carrier with a flow of 0.225 mL/s. The samples were diluted in ethanol before being analysed by GC. The two different reactor designs were used in order to compare their results.

HSAG-100 was gently supplied by Bodio (Switzerland) and it was used as a catalyst. The catalyst was characterized by nitrogen physisorption using the BET method, temperature-programmed desorption (TPD) coupled to mass spectrometry, scanning-electron microscopy (SEM) with X-ray microanalysis, transmission-electron microscopy (TEM) and X-ray diffraction (XRD).

3.8.2 Results and Discussion

Characterization of High Surface Area Graphite (HSAG-100)

SEM with X-ray microanalysis

The ash content of HSAG-100 was initially intended to be determined by an ASTM method (C561-91), which basically consisted of determining weight differences

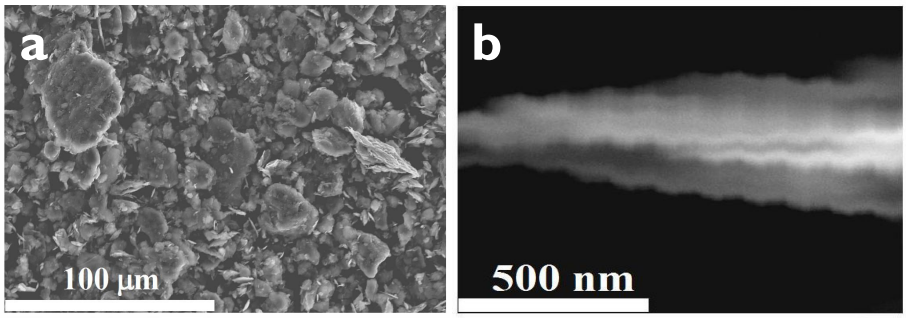

Figure 3.8.1 SEM images of HSAG-100.

before and after placing the sample holder in a muffle furnace under a slow stream of air and heating the sample up to 750 °C. Nevertheless, we did not succeed, since a hard layer was formed over the graphite and no further combustion was allowed. Therefore, an alternative method to determine ash content was needed. SEM with X-ray microanalysis was able to provide the required information. The spectrum (Fig. 3.8.2) proved the ash lack in HSAG-100, since the only elements detected were

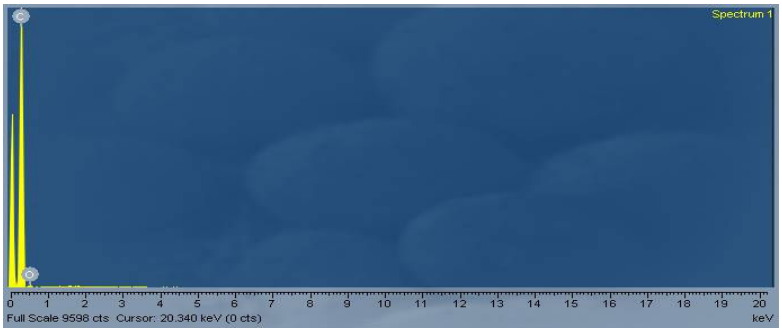

Figure 3.8.2 X-ray microanalysis spectrum of HSAG-100.

carbon and oxygen. Moreover, the micrographs showed the morphological appearance of HSAG-100. One of them (Fig. 3.8.1, a) was performed at lower magnification values and presented the broad range of the particle size. The micrograph (b) was performed with a higher magnification value, what allowed us to distinguish the characteristic ordered-layer structure of graphite. It also showed that this graphite had a high purity.

TEM

The striped regions in the picture (Fig. 3.8.3) strengthened the observations of layered structure carried out by SEM analysis. The intra-layered distance was not higher than 7 nm.

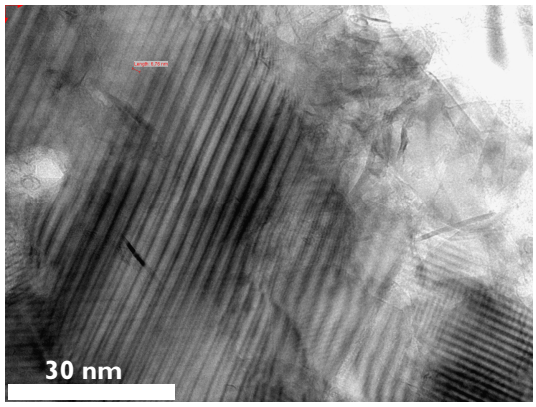

Figure 3.8.3 TEM image of HSAG-100.

TPD measurements

The surface chemistry of the material was determined by coupling a mass spectrometer to the outlet of a TPD system. The resulting plot (red line) is shown in Fig. 3.8.4 and presented an extremely broad and low peak from 100 °C to 800 °C. The amount of eluted gases was much lower than AC indicating that HSAG-100 had much less oxygen surface groups than AC. In order to evaluate such difference, the resulting plot shows also the TPD measurement for AC (green line). This result was in good agreement with the data obtained by X-ray microanalysis [6-8].

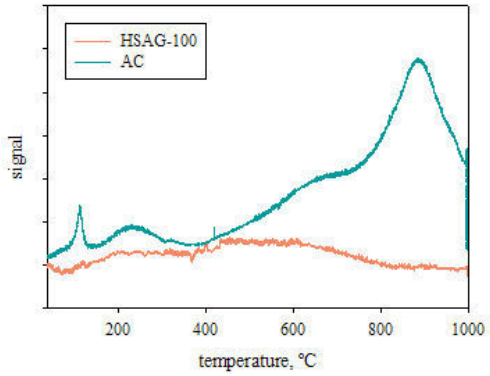

Figure 3.8.4 TPD profile of HSAG-100 (red line) and AC (blue line).

It is then remarkable the lack of surface functionality exhibited by the graphite HSAG-100, that must be taken into account for the proposal of a mechanism for the non-oxidative catalytic dehydrogenation.

Physisorption of nitrogen

For common graphite, the surface area and the pore size distribution are usually of minor importance. Nevertheless, HSAG-100 presented a relatively high surface area, probably because of previous chemical or mechanical treatments. The isotherm plot (Fig. 3.8.5) corresponded to a type II sorption isotherm, according to the BDDT

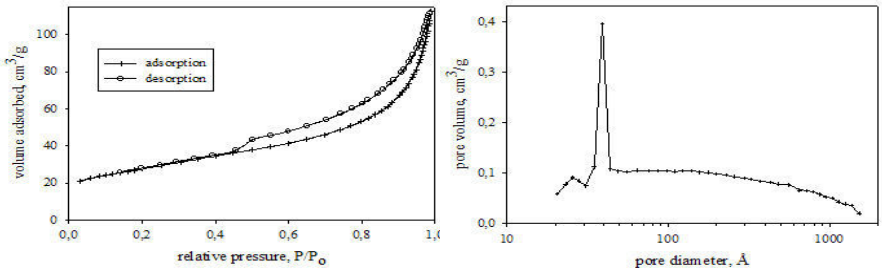

Figure 3.8.5 Isotherm (left) and BJH desorption dV/dlog(D) pore volume (right) plots of HSAG-100.

classification Its hysteresis loop is classified as type H_3, according to IUPAC Type H_3 loops are usually given by aggregates of plate-like particles or adsorbents containing slit-shaped pores [9, 10]. Its surface area calculated with BET method is 103 m^2/g.

The pore-size distribution plots, obtained according to the Barrett-Joyner-Halenda (BJH) method are also shown in Fig. 3.8.5. The predominant pore diameter for HSAG-100 was at 3.9 nm. The pore size distribution was quite narrow and proved the mesoporosity and lack of microporosity of the material.

XRD measurements

The XRD pattern of HSAG-100 (Fig. 3.8.6) showed the characteristic reflection peaks of graphite (JCPDS 08-0415, graphite, blue lines). The crystallite size was calculated by TOPAS [11] and gave a value of 15 nm. Since the value was lower than 30 nm, this graphite was considered to be microcrystalline [12]. By observing SEM images and the crystallite size, HSAG-100 was determined to be polycrystalline, as most of graphitic materials [12].

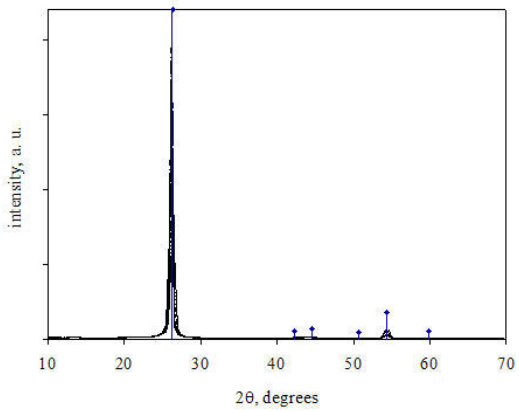

Figure 3.8.6 XRD pattern of HSAG-100.

3.8.3 Catalytic Activity

Analogously to the results of AC at 200 °C (see *Chapter 3.7*), tri-unsaturated FAEE were also detected for this case, using HSAG-100 as a catalyst and the old reactor design (see *Chapter 2.1*). A sieving procedure was performed to the material in order to get several fractions in the following ranges: 1-100 μm, 100-150 μm, 150-

200 μm and 200-500 μm, and to study the influence of the particle size to the catalytic behaviour of HSAG-100. Not only the total conversion (Fig. 3.8.7) value, but also the selectivity values (Fig. 3.8.8) toward the different compound families, were similar for all pellet sizes except the fraction of 200-500 μm, which presented slightly different selectivity values. Unlike the former studies with AC as catalyst, new compound peaks were detected by GC. Those compounds did all elute at lower retention times indicating that they were more volatile compounds. This fact was probably due to a shortening of the hydrocarbon chain molecules. In fact, GC-MS analysis (see Annex III) confirmed that those new compounds corresponded to shorter molecules, such as, ethyl myristate or decadienal (Fig. 3.8.9), thus, they were products of a *cracking* reaction, which did not happen with AC. Snare et al. [13] reported also the pyrolysis of stearic acid when using carbon based catalysts for the deoxygenation reaction.

Concerning the total conversion of ethyl linoleate at 200 °C, the value achieved for all pellet sizes was around 30 %. Considering that the surface area of HSAG-100

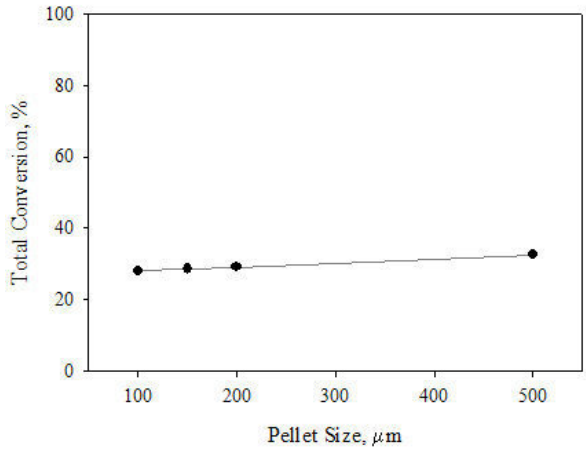

Figure 3.8.7 Total conversion of ethyl linoleate vs. pellet sizes at 200 °C

is approximately 14 times lower than the surface area of AC, and then HSAG-100 came out to be much more active than AC, as far as the specific activity per active site is concerned.

Regarding the selectivity values, more than 50 % (≈ 62 %) of the converted material suffered cracking giving place to the different products shown in Fig. 3.8.8. In the case of 200-500 μm fraction, the cracking selectivity had a lower value of 57

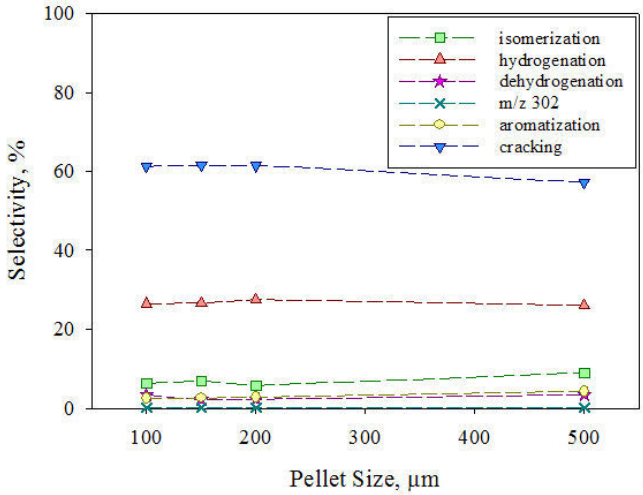

Figure 3.8.8 Selectivity values vs. pellet sizes at 200 °C.

%. Mono-unsaturated FAEE obtaining represented a 26 % of converted starting material, while the selectivity towards tri-unsaturated and aromatic FAEE had both a similar value around 3.5 %, excepting the fraction of 200-500 μm; in this case, the selectivity towards aromatic FAEE was slightly higher achieving 4 %. The hydrogen produced in the dehydrogenation reaction, which was a product in the formation of aromatic and tri-unsaturated FAEE, was not enough to give place to a hydrogenation selectivity value of 26 %. Thus, it is possible that some cracking reaction gave hydrogen as a reaction product. The reaction of isomerization gave a selectivity value around 6 % and 9% for all ranges and for the range between 200 μm and 500 μm, respectively. Therefore, in comparison to AC, isomerization, hydrogenation and aromatization reactions were less favourable in the case of HSAG-100. However, the cracking reaction turned out to be qualitatively important and became the differential point between the two catalysts.

The responsible for the dehydrogenation activity of graphite may not be able to be associated to its oxygen-containing surface groups, because they were practically

absent. In oxidative dehydrogenation reaction, it was proposed that the strongly basic chinoidic surface functionalities, generated as resonance stabilized C=O surface terminations of the edge/kink regions (prismatic planes) and accountable for dehydrogenative properties, were formed during the induction period in the catalytic testing [5, 14]. However, the catalytic performance of this material under non-oxidative conditions should be considered in order to a better understanding of the reaction mechanism. Consequently, the activity should be related to another different aspect of this catalyst and/or, even, to the cracking-resulting molecules, since most of them appeared to be totally saturated.

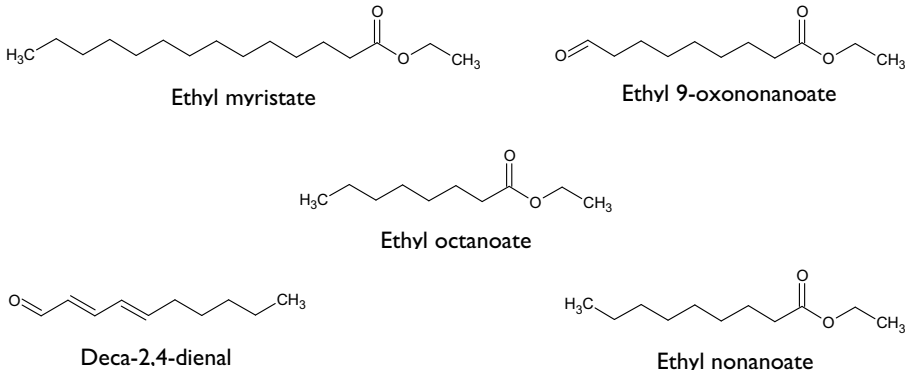

Figure 3.8.9 Main compounds resulting of cracking reaction detected by GC-MS.

3.8.4 Conclusions

No ash content was detected, so carbon and oxygen were the main components of HSAG-100. It had a much lower amount of oxygen-containing surface groups in comparison to AC.

It rendered a higher total conversion of ethyl linoleate than AC, if considering conversion relative to surface area. Analogously to AC, di-unsaturated FAEE, mono-unsaturated FAEE, aromatic FAEE were detected as reaction products. The decrease of reaction temperature to 200 °C allowed us to detect tri-unsaturated FAEE. However, some products from cracking reactions gave a selectivity value around 60 %.

The different fractions of HSAG-100 obtained by sieving yielded a similar catalytic behaviour, except that between 200-500 μm. This fraction gave slightly different values in the obtaining of tri-unsaturated FAEE, aromatic FAEE, isomerization FAEE and cracking products.

Dehydrogenation reaction products were detected by using oxygen-free-surface catalyst, such as HSAG-100, under non-oxidative conditions. This observation may introduce a new consideration in the proposed mechanism of dehydrogenation utilizing graphitic materials.

References

[1] M. F. R. Pereira, J. J. M. Órfão, J. L. Figueiredo, Colloids Surf. A 241 (2004) 165.
[2] M. F. R. Pereira, J. J. M. Órfão, J. L. Figueiredo, Carbon 42 (2004) 2807.
[3] N. Maksimova, G. Mestl, R. Schlögl, Stud. Surf. Sci. Catal. 133 (2001) 383.
[4] N. I. Maksimova, V. V. Roddatis, G. Mestl, M. Ledoux, R. Schlögl, Eurasian Chem. Tech. J. 2 (2000) 231.
[5] G. Mestl, N. I. Maksimova, N. Keller, V. V. Roddatis, R. Schlögl, Ang. Chem. Int. Ed. 40 (2001) 2066K.
[6] M. F. R. Pereira, J. J. M. Órfão, J. L. Figueiredo, Appl. Catal. A 184 (1999) 153.
[7] M. F. R. Pereira, J. J. M. Órfão, J. L. Figueiredo, Appl. Catal. A 196 (2000) 43.
[8] A. L. Dantas Ramos, P. da Silva Alves, D. A. G. Aranda, M. Schmal, Appl. Catal. A 277 (2004) 71.
[9] K. S. W. Sing, D. H. Everett, R. A. W. Haul, L. Moscou, R. A. Pietotti, J. Rouquerol, T. Siemienieska, Pure Appl Chem 57 (1985) 603.
[10] F. Rouquerol, J. Rouquerol, K. Sing, in: Adsorption by powders and porous solids, Academic Press, San Diego, USA, 1999.
[11] TOPAS 31 *General profile and structure analysis software for powder diffraction data User's manual*, Bruker AXS GmbH, Karlsruhe, Germany.
[12] M. Wissler, J. Power Sources 156 (2006) 142.
[13] M. Snåre, I. Kubičková, P. Mäki-Arvela, K. Eränen, D. Yu. Murzin, Ind. Eng. Chem. Res. 45 (2006) 5708.
[14] D. S. Su, N. Maksimova, J. J. Delgado, N. Keller, G. Mestl, M. J. Ledoux, R. Schlögl, Catal. Today 102-103 (2005) 110.